www.ijbar.org

ISSN 2249-3352 (P) 2278-0505 (E)

Cosmos Impact Factor-5.86

Flywheel Storage system based Microgrid with MMC-HVDC Grid Integration and It's FRT capability Enhancement

Mekala Rajkumar, K. Ranjith Kumar
1, PG Scholar, Department of Electrical and Electronics Engineering
2, Assistant Professor, Department of Electrical and Electronics Engineering
Vaagdevi College of Engineering, Bollikunta, Warangal (Dt), TS, India.
razkumar.mekala@gmail.com

Abstract: This article presents a Proportional-Resonant (PR) based control method for improving the fault ride-through (FRT) capabilities of Modular Multilevel Converter (MMC) based High Voltage Direct Current (HVDC) transmission networks, which integrate renewable energy resources (RERs) from remote locations. The intermittent nature of RERs and symmetrical/asymmetrical low-voltage faults on the AC side can create operational challenges, reducing the MMC's power transmission capability and increasing HVDC link voltage. To address power fluctuations from RER intermittency, unexpected load changes, and low-voltage issues at the point of common coupling (PCC) in AC grids, the proposed control method uses a flywheel energy storage system (FESS) within PV-wind-MMC-HVDC setups to stabilize HVDC link voltage, eliminating the need for dynamic braking resistors (DBR) and allowing seamless RER integration. This approach also minimizes reductions in renewable energy output during low-voltage events. Tested under symmetrical and asymmetrical low-voltage faults, and validated through variations in wind speed, solar irradiance, and temperature, the PR-based control strategy effectively manages excess HVDC link energy and enhances the resilience of the MMC-HVDC network.

Key words: Modular multilevel converter, high voltage direct current, Renewable energy resources, Fault ride-through, point of common coupling and flywheel energy storage.

I. Introduction

The integration of renewable energy resources (RERs) into high-voltage direct current (HVDC) networks is gaining traction due to the inherent benefits of Modular Multilevel Converters (MMCs) in Voltage Source Converter (VSC)-HVDC systems. These converters are compact, scalable, and adaptable, making them ideal for connecting renewable sources like wind and solar to the grid, especially in remote areas. MMC-HVDC systems provide crucial support to the AC grid by managing frequency and offering dynamic voltage control, both of which are essential for maintaining grid stability with intermittent renewable sources. Yet, achieving seamless integration remains challenging, primarily due to the limited fault ride-through (FRT) capabilities of MMC-HVDC networks.

During grid faults, such as voltage dips or short circuits, wind farms are often unable to transmit their full power output. The active power transmitted by the onshore MMC can drop drastically, leading to an imbalance in the HVDC system. As the DC link tries to absorb

www.ijbar.org

ISSN 2249-3352 (P) 2278-0505 (E)

Cosmos Impact Factor-5.86

the excess energy, the voltage across the DC link rises rapidly as capacitors charge, creating an overvoltage issue. Managing this overvoltage is critical, as it can affect the stability of the entire system and, if unchecked, may result in equipment damage or loss of renewable energy generation.

Traditional methods for handling this challenge include reducing wind farm output to mitigate power flow or using dynamic braking resistors (DBRs) to dissipate the excess energy in the HVDC link. While effective, these methods are hardware-intensive, requiring additional components such as brake resistors, DC choppers, and power switches configured in series-parallel arrays. This hardware can increase system complexity, costs, and maintenance requirements, which are already substantial in HVDC installations. Additionally, the reliance on braking systems and power flow reduction means that renewable energy generation may need to be curtailed during fault events, limiting the efficiency and utilization of clean energy sources.

Alternative control strategies, such as frequency modulation, voltage droop control, and communication-based de-loading, have been explored to dynamically manage power flow without heavy reliance on hardware. In frequency modulation, the offshore grid frequency is increased to manage DC voltage, but this technique is limited by the insufficient df/dt tolerance of wind farms and their slower response in adjusting active power. Voltage droop control can help with FRT by facilitating a quick reduction in wind farm output during faults, but this method also has its constraints. Communication-based de-loading offers promise by coordinating adjustments in renewable generation through DC-link communication, yet it suffers from potential communication delays and reliability issues, particularly in large offshore wind farms.

Energy storage systems (ESS) are increasingly viewed as a practical solution to address these limitations and support RER integration into HVDC networks. Various ESS technologies, including Battery Energy Storage Systems (BESS), lithium-ion batteries, supercapacitors, and flywheel energy storage systems (FESS), can help mitigate the intermittency of renewable sources and enhance grid stability. Lithium-ion batteries, for instance, have high energy density and efficiency, making them suitable for sustained energy storage. However, their limited power density can restrict their effectiveness during high-power surges, and frequent cycling can degrade their performance over time.

Supercapacitors offer high power density and rapid response times, ideal for situations requiring quick energy release, such as fault conditions. Yet, they are expensive, prone to self-discharge, and generally less suited for prolonged energy storage, making them less ideal for large-scale, high-capacity applications. Flywheel energy storage systems, on the other hand, provide a promising alternative. FESS units can rapidly store and release kinetic energy, helping to balance the HVDC link voltage during grid faults without degradation over repeated cycles. This fast dynamic response makes FESS particularly effective for stabilizing DC-link voltage and addressing FRT issues, reducing the need for DBRs and preventing the need to curtail renewable generation.

www.ijbar.org

ISSN 2249-3352 (P) 2278-0505 (E)

Cosmos Impact Factor-5.86

Despite the potential of flywheels, challenges remain, especially in scaling up to the capacity required for large HVDC applications. High-capacity induction motors are needed for flywheels to handle large energy loads, but their availability at scale is limited, which complicates large-scale deployments. Additionally, existing studies on FESS integration have not extensively addressed unbalanced fault conditions or rapid AC load changes, which are common in real-world grid operations.

This research aims to fill these gaps by investigating the use of MMCs in connecting flywheel energy storage systems to HVDC networks and assessing their effectiveness in enhancing FRT capability. Specifically, it evaluates the role of FESS in stabilizing DC-link voltage during low-voltage events, including both symmetrical and asymmetrical faults, as well as in conditions of fluctuating renewable energy output due to variable wind or solar input. The objective is to provide a more comprehensive approach to integrating energy storage with MMC-HVDC networks that can manage transient disturbances without compromising RER output or requiring complex hardware additions.

The study's findings could help establish a more robust and resilient MMC-HVDC framework, allowing renewable energy sources to be fully utilized even during fault events. By incorporating flywheel energy storage, the HVDC link can maintain stability, potentially enabling further renewable integration on a larger scale while minimizing the dependency on traditional hardware solutions for overvoltage protection. This approach supports a pathway to more sustainable and efficient energy systems, where renewable generation is not only feasible but also reliable, resilient, and capable of supporting grid stability across diverse operational conditions.

II. System Modeling And Controller Design

Figure 1 depicts the system's main components, which include wind and solar farms linked to a permanent magnet synchronous motor-based flywheel energy storage device. The MMC2 regulates the voltage on the HVDC-link, whereas the MMC1 controls the AC grid and the PV-wind system in this configuration. Additionally, MMC3 incorporates PMSM and flywheel energy storage in the process of establishing the AC grid. System capacity can be increased by a single unit of energy storage and renewable energy through the use of a regulated current source and multiplier.

a) Integrating Off-Grid Power Generation with MMC2 and MMC1

The primary goal of controlling solar and wind energy converters is to facilitate their integration into the AC grid established by MMC2. The maximum output power of the photovoltaic panel changes with temperature and changes in sun illumination, as seen by the power-voltage (P-V) characteristic curve. As operational circumstances (sun irradiation and temperature) change, the controller of the PV side converter adjusts the DC-link voltage using the modified incremental conductance approach to optimise the power output of the photovoltaic system. For further details on potential grid integration of solar electricity, see

www.ijbar.org

ISSN 2249-3352 (P) 2278-0505 (E)

Cosmos Impact Factor-5.86

references [9]. The maximum power that can be produced by wind energy is dependent on the wind speed. Using field-oriented control, the reference electromagnetic torque can be followed from the optimal wind energy point. To learn more about the specifics of how wind energy networks that use DFIG can be integrated, see references [9]. The HVDC-link voltage is controlled by MMC1, and the photovoltaic-wind system is connected to the AC grid by MMC2. The full design can be found in references.

b) Flywheel Management Use of a PMSM System

While MMC1 regulates the HVDC link voltage, MMC3 generates the AC voltage for the PMSM-based flywheel integration. The grid side converter (GSC) gets the reference power command when there are low voltage disturbances at PCC1, changes to the load, or variations in renewable energy. By adjusting the amount of electromagnetic torque it produces using field-oriented control (FOC), a permanent magnet synchronous motor (PMSM) can transition between driving and generating an electric current.

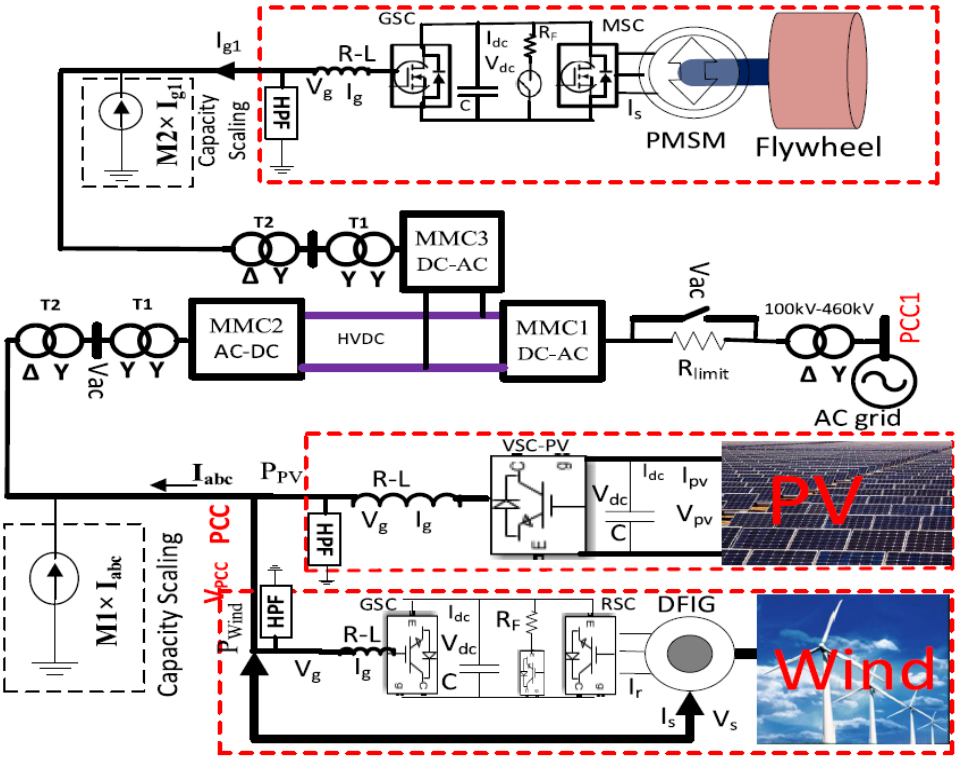

Figure 1 MMC-HVDC system

The flywheel stores energy when driving by increasing the speed of the rotor and flywheel, and releases it when operating the generator by decreasing the speed of the rotor and flywheel. The PMSM stator current is governed by the following equation in the rotor-field dq coordinate system.

$$\left(\mathrm{L_d}\frac{di_d}{dt} + R_s i_d\right) = \mathrm{L_q}\omega i_q + V_d$$

www.ijbar.org

ISSN 2249-3352 (P) 2278-0505 (E)

Cosmos Impact Factor-5.86

$$\left(\mathrm{L_q}\frac{di_q}{dt}+R_s i_q\right)=-\mathrm{L_d}\omega i_d-\lambda_{\mathrm{m}}\omega+V_q$$

Permanent Magnet Synchronous Motors (PMSMs) rely only on encoders to determine the rotor flux location, in contrast to squirrel cage and doubly fed induction motors. A Permanent Magnet Synchronous Motor (PMSM) can run without reactive power from outside sources. This causes the MSC's reactive current to remain constant at zero. In order to get dq current, the stator phase current is angled relative to the rotor flux location.

$$T_e=\frac{3}{2}\lambda_{\mathrm{m}}Pi_q$$

Proves that the electrical torque is governed by the q-axis current and that the reactive current is zero. Indirectly controlling the electromagnetic torque and the speed of the flywheel, the DC link voltage regulation loop generates the current along the q-axis. The MSC's current controller has been set up. The PMSM side converter's control is shown in Figure 3.2 (d). To create the MSC's dq axis voltage, a PI controller (PI1) handles any current variation and then adds the decoupling term. The voltage on the dq axis is used in conjunction with the rotor flux angle to generate the modulating signal, abcsignal. An axle connects the flywheel to the rotor of a permanent magnet synchronous motor. Therefore, the flywheel speed is proportional to the rotor speed of the PMSM.

c) Energy Management System

The HVDC-link voltage is increased due to the reduced power transfer capacity of the MMC1 caused by the low voltage defect at the PCC1. In order to keep the HVDC-link voltage within certain limits and to waste excess energy, the dynamic brake resistor is typically placed in parallel with the gearbox line. During the three-line-to-ground (LLLG) breakdown at the PCC of the AC grids, multiple series-parallel combinations of semiconductor switches are needed to discharge a significant quantity of HVDC power.

www.ijbar.org

ISSN 2249-3352 (P) 2278-0505 (E)

Cosmos Impact Factor-5.86

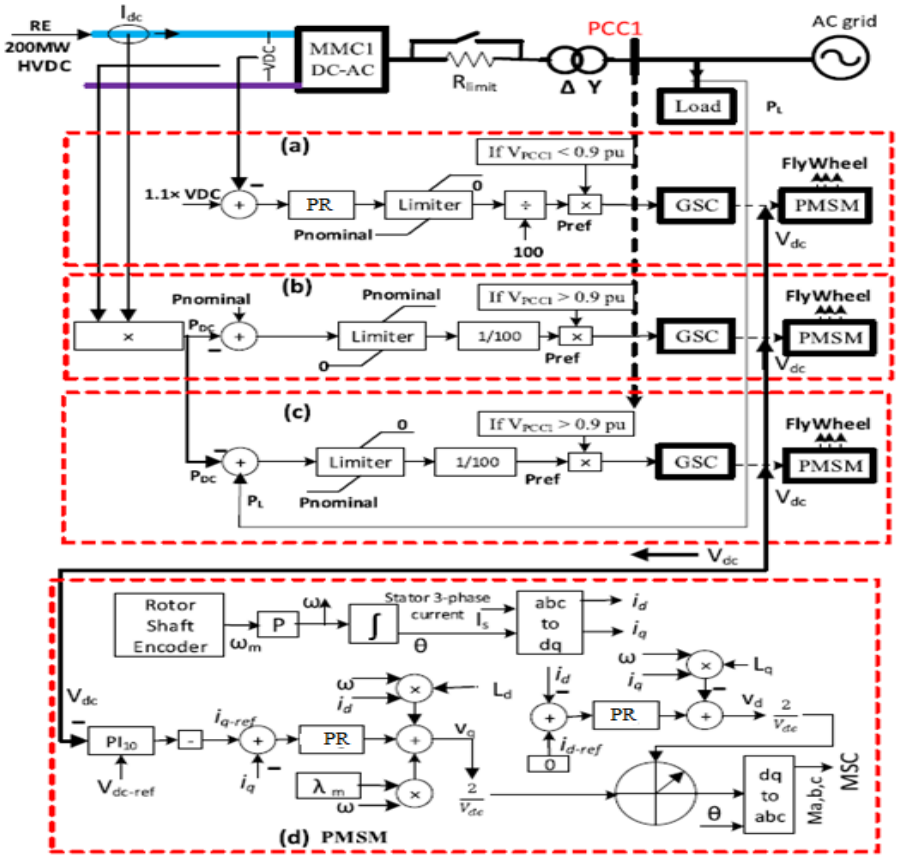

Figure 2 Control strategy (a) energy control (b) power leveling control (c) Regulation of excess power (d) Control of the machine-side converter

The real power flow could be affected by changes in the HVDC connection voltage caused by the dynamic brake resistor's multiple switchings. The intermittent nature of solar and wind power is characterised by its sensitivity to changes in temperature, wind speed, and solar radiation. As a result, energy storage using flywheels has been considered as a way to reduce the intermittent nature of renewable power, calm down fast transients caused by AC side low voltage disturbances, and soak up excess power during AC side sudden changes in load. Furthermore, the DBR is removed from the system by means of a flywheel.

d) AC Side Low Voltage Faults at Pcc1

The HVDC connection voltage rises because MMC1's capability decreases when PCC1 experiences low voltage difficulties. Therefore, the flywheel needs to receive the excess energy from the HVDC link. The error is handled by the controller (PI1), which determines the reference power instruction for the grid side converter (GSC) when the HVDC link voltage is greater than 1.1pu and the PCC voltage is less than 0.9pu, as shown in Figure 2(a). The GSC operates by continuously regulating power. A higher DC link voltage results from the GSC injecting power into the DC link. The PI controller, depicted in Figure 2(d), controls the DC link voltage and manages any voltage variation. This current, known as the

www.ijbar.org

ISSN 2249-3352 (P) 2278-0505 (E)

Cosmos Impact Factor-5.86

reference quadrature axis current (Iq−ref) or electromagnetic torque management current in the PMSM-connected flywheel, is produced by the controller. By increasing the speed of the flywheel, the excess energy from the HVDC link can be stored. Therefore, the HVDC link voltage stays within the allowed range.

The control operation improves the intermittency of renewable energy sources when operating at standard grid voltage, as shown in Figure 2(b). The entire amount of energy generated by renewable sources and fed into the MMC1 is known as the nominal power of renewable energy (Pnominal). Because of the flywheel energy storage device, any deviation from the nominal power is reduced. A reference power command for the GSC is the difference between the nominal power of renewable energy and the real HVDC link power (PDC), as shown in Figure 2(b). The GSC is involved in transporting energy from flywheel storage to the HVDC link via the MMC3 in this instance. As a result, the GSC's DC link voltage drops. Figure 2(d) shows the PI controller, which is responsible for regulating the DC link voltage and managing the fluctuation in that voltage. This variation in turn generates the reference quadrature axis current (Iq−ref) or the current needed to control the electromagnetic torque in the PMSM-connected flywheel. Discharging the required extra energy slows down the flywheel. So, even though renewable energy is affected by meteorological conditions (temperature, wind speed, and sun radiation), the MMC's power supply is constant.

(e) Varying loads

There will be a power disparity between the power flowing into the HVDC link and the power being used when the AC grid experiences a sudden load interruption at normal voltage. Control mechanism shown in Fig. 2(c) then directs the differential power to the flywheel energy storage. For the GSC, the disparity is like a reference power command. A higher DC link voltage results from the GSC injecting power into the DC link. The PI controller, depicted in Figure 2(d), controls the DC link voltage and manages any voltage variation. This current, known as the reference quadrature axis current (Iq_ref) or electromagnetic torque management current in the PMSM-connected flywheel, is produced by the controller. To store excess energy from the HVDC link caused by sudden changes in load, the flywheel's speed is increased.

(f) Flywheel

According to reference, the amount of kinetic energy stored in the flywheel is determined by its moment of inertia J (kgm−2) and the square of the angular velocity ω (rad/sec). An important design feature of flywheels is their moment of inertia, which is affected by the flywheel's shape and mass m (kg). In order to ensure safe functioning, the flywheel's angular velocity, denoted as ωfw, is limited to a minimum (ωmin) and maximum (ωmax) value.

www.ijbar.org

ISSN 2249-3352 (P) 2278-0505 (E)

Cosmos Impact Factor-5.86

$$E_{fw} = \frac{1}{2} J \omega^2$$

$$H_{fw} = \frac{E_{fw}}{MVA_{rated}} \text{MWs/MVA}$$

$$E_{fw(available)}(Wh) = \frac{1}{3600}\left(\frac{1}{2} J \omega_{max}^2 - \frac{1}{2} J \omega_{min}^2\right)$$

$$\begin{aligned} &SOE_{fw}(t) \\ &= SOE_{fw}(t - \Delta T) - \frac{\Delta T}{3600 \times E_{max}}\left(\frac{P_{fw}}{\eta_{fw}} + K_{fr}\omega\right) \\ &= SOE_{fw}(t - \Delta T) - E_{con} \end{aligned}$$

The flywheel energy storage system's capacity can be reduced in relation to the total renewable energy due to the speed that results from absorbing surplus energy from the HVDC link. Capacity needs to be increased to handle variations in load and swings in renewable energy production. The flywheel's dimensions can change based on the required support.

III. Simulation Result Discussion

The MMC controller has a sampling time of 100 microseconds. Having said that, the PV, Wind, and Flywheel controllers all have sample times of 50µs. Due to the system's complexity, a multi-rack RTDS platform was utilised for its development. For its hardware platform, the RTDS multi-rack relied on Nova Core and PB5 CPUs. In contrast to Rack-1's MMC1 and MMC3 with flywheel, Rack-2's MMC2 features PV and wind power. Using the dSPACE-SCALEXIO controller, the MMC1 controller was put into place. Images 3, 4, and 5 show the dSPACE-RTDS hardware installations, the MMC1controller signal in the dSPACE controller, and the RTDS runtime interface, respectively. It was possible to model a 200 MW PV-Wind system by reducing the input current to the PCC terminals from a 1.74 MW PV array and one 2 MW wind generating unit. A 200MW flywheel energy storage system was built in a similar vein by expanding a 2MWvand 3.5MWs/MVA PMSM based system. Tables 1–3 of the appendix provide all the necessary information on the MMC-HVDC-flywheel energy storage system used in this research.

Due to its size and complexity, the power system network is vulnerable to issues with low voltage. The converter's power transmission performance drops dramatically at low voltage, causing the HVDC connection voltage to rise. So, to control the additional energy for the HVDC voltage regulation, a suitable protection system is required. The conventional controller for regulating the voltage of the HVDC connection during low voltage failures often makes use of dynamic brake resistors to dissipate the excess energy in the link. The HVDC link voltage is controlled by the proposed work without the DBR. In order to ensure that the flywheel energy storage controller could keep the HVDC-link voltage for the PV-

www.ijbar.org

ISSN 2249-3352 (P) 2278-0505 (E)

Cosmos Impact Factor-5.86

wind coupled MMC-HVDC network under the specified threshold, the severe balanced and unbalanced faults were applied at PCC1.

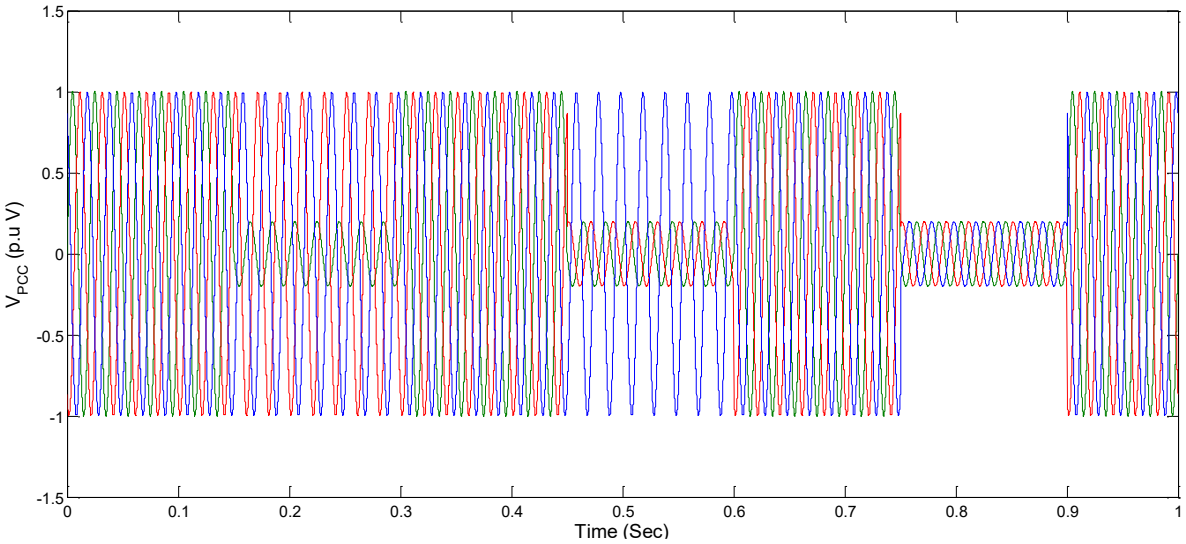

Figure 3 80% voltage decrease at different faults

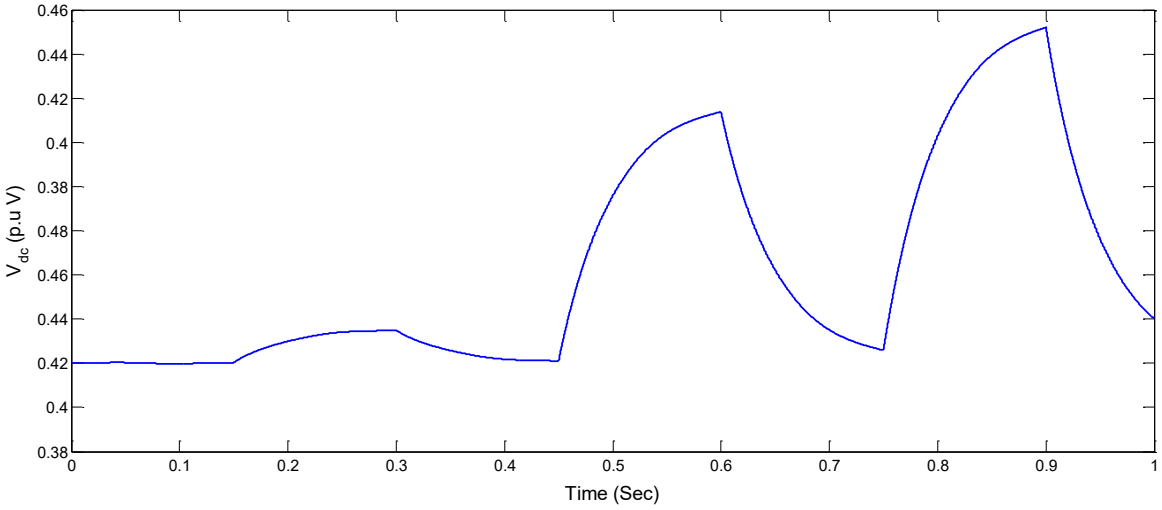

Figure 4 DC link voltage

Although PV and wind generation were unaffected by the fault at PCC1, the excess energy from the HVDC-link was absorbed by the flywheel energy storage. Figure 3 shows that at 0.7s, 1.6s, and 2.6s, respectively, a single line to ground (LG) fault, a double line to ground (LLG) fault, and a three phase to ground (LLLG) fault are introduced to PCC1. These faults each last 500ms. As a result of these failures, the PCC1 voltage drops eighty percent. The true power of MMC1 is reduced to a minimum during the three-phase to ground failures at PCC1.

www.ijbar.org

ISSN 2249-3352 (P) 2278-0505 (E)

Cosmos Impact Factor-5.86

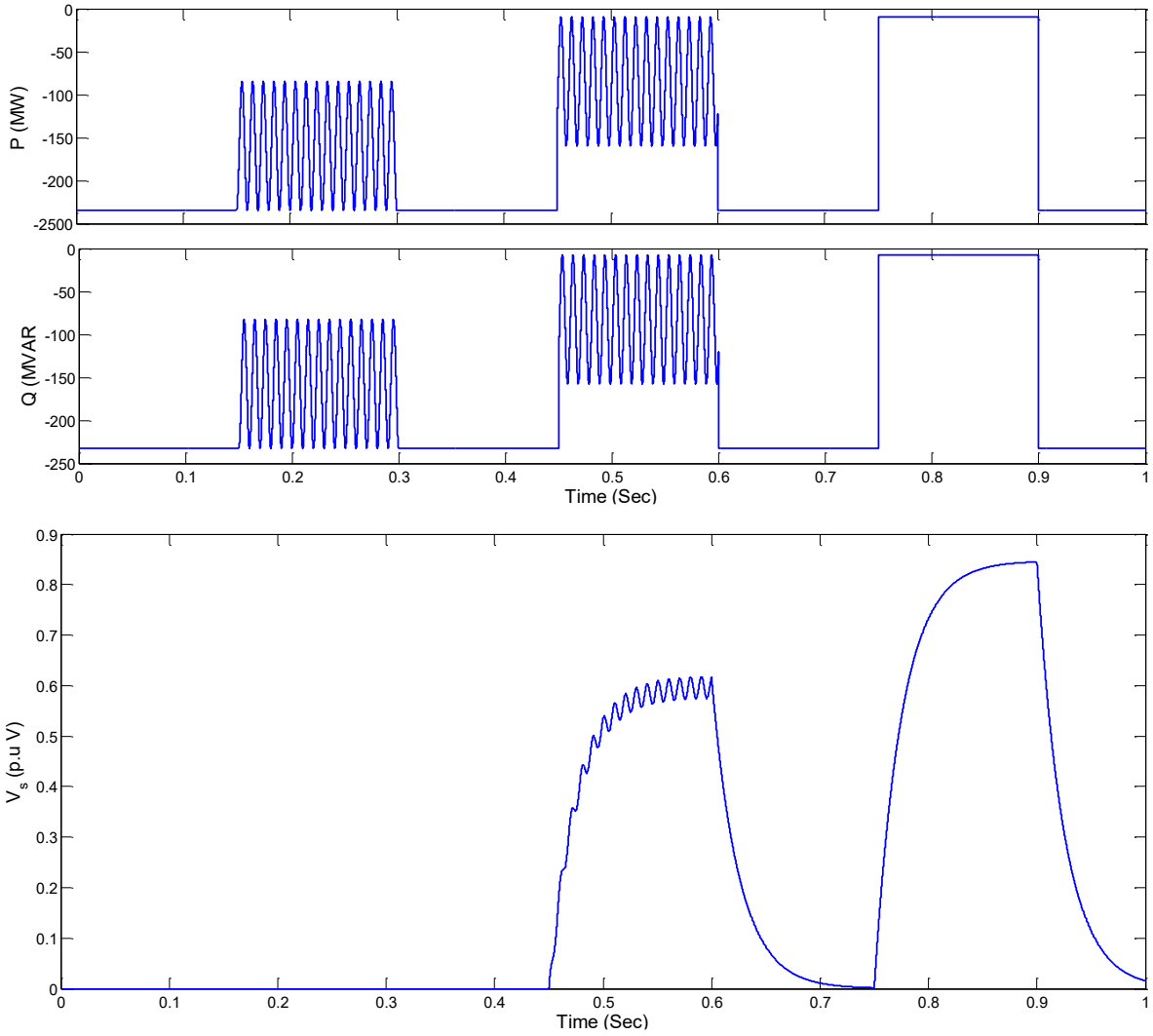

Figure 5 Real power, reactive power, and voltage under faults

Similarly, a 500ms duration single line to ground fault (LG), double line to ground fault (LLG) and three-phase to ground fault (LLLG) is introduced to PCC1 at 0.7s, 1.6s and 2.6s correspondingly, as indicated in Fig. 4 However, the PCC1 voltage is dropped by 50% during these breakdowns.

In addition, a 500ms length line to line fault (LL), is introduced to PCC1 at 0.7s, as indicated in Fig. 5 However, the PCC1 voltage reduction is not symmetrical, and reduced by 40% to 70% during this malfunction.

www.ijbar.org

ISSN 2249-3352 (P) 2278-0505 (E)

Cosmos Impact Factor-5.86

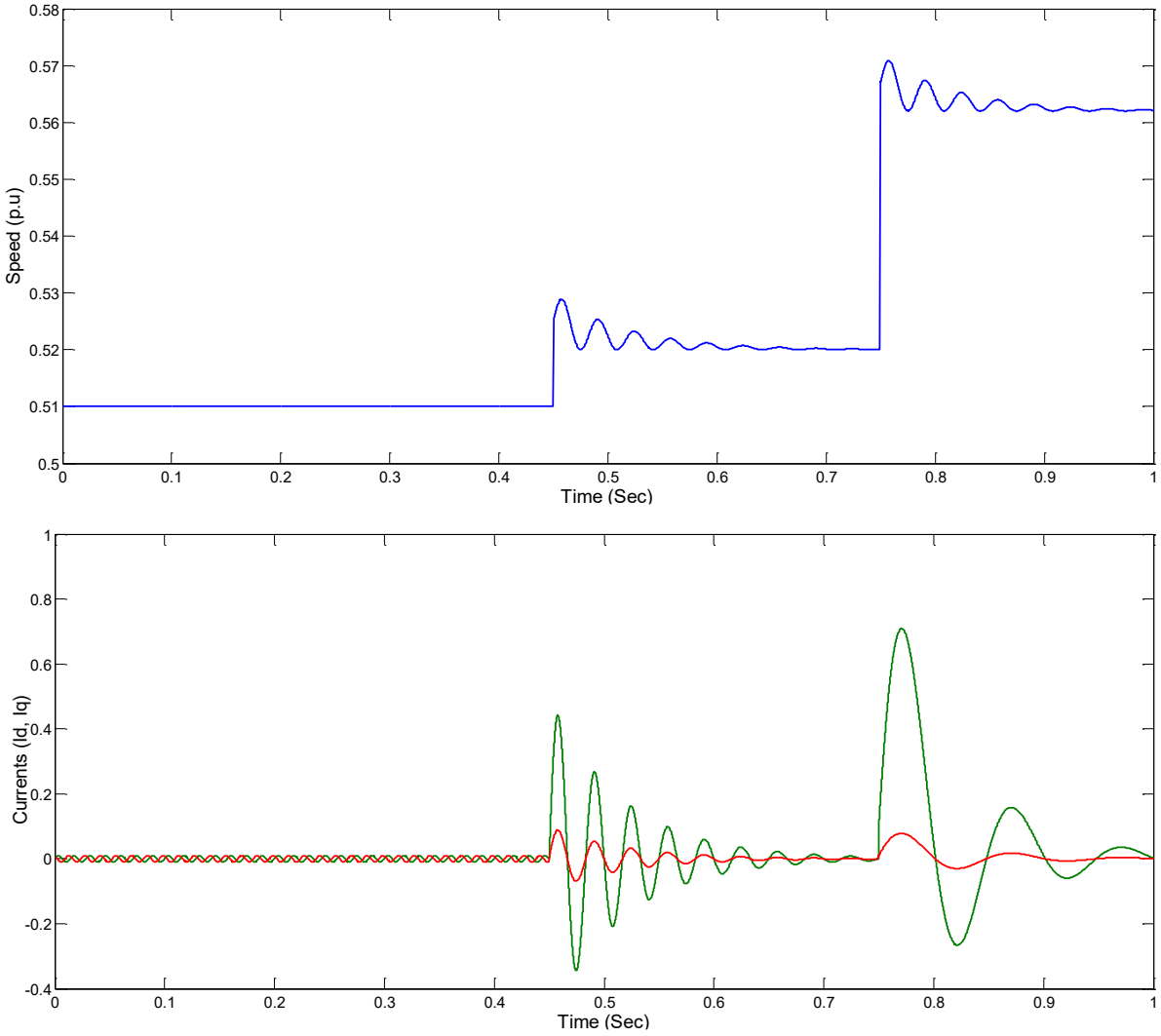

Figure 6 Injected Currents and speed under Fault

IV. Conclusion

The Proportional-Resonant (PR) based control method demonstrates significant potential in enhancing the fault ride-through (FRT) capabilities of MMC-based HVDC networks that integrate renewable energy resources from remote locations. By employing a flywheel energy storage system (FESS) to manage voltage stability on the HVDC link, the method effectively addresses operational challenges related to RER intermittency, load variations, and low-voltage conditions on the AC side. This approach not only reduces the reliance on dynamic braking resistors (DBR) but also ensures uninterrupted renewable energy integration, even during low-voltage faults. The successful performance of the PR-based control method under various fault scenarios and environmental conditions confirms its effectiveness in stabilizing power fluctuations, thereby enhancing the resilience and efficiency of MMC-HVDC systems in renewable energy applications.

References

ISSN 2249-3352 (P) 2278-0505 (E)

Cosmos Impact Factor-5.86

[1] M. I. Hossain and M. A. Abido, ‘‘SCIG based wind energy integrated multiterminal MMC-HVDC transmission network,’’ *Sustainability*, vol. 12, no. 9, p. 3622, Apr. 2020, doi: 10.3390/SU12093622.

[2] M. I. Hossain and M. A. Abido, ‘‘Positive-negative sequence current controller for LVRT improvement of wind farms integrated MMC-HVDC network,’’ *IEEE Access*, vol. 8, pp. 193314–193339, 2020, doi: 10.1109/ACCESS.2020.3032400.

[3] M. I. Hossain and M. A. Abido, ‘‘Active power control of PV-battery connected MMC-HVDC system for FRT support,’’ *Appl. Sci.*, vol. 10, no. 20, p. 7186, Oct. 2020, doi: 10.3390/APP10207186.

[4] M. Zhang, X. Yuan, and J. Hu, ‘‘Inertia and primary frequency provisions of PLL-synchronized VSC HVDC when attached to islanded AC system,’’ *IEEE Trans. Power Syst.*, vol. 33, no. 4, pp. 4179–4188, Jul. 2018, doi: 10.1109/TPWRS. 2017.2780104.

[5] J. N. Sakamuri, Z. H. Rather, J. Rimez, M. Altin, O. Goksu, and N. A. Cutululis, ‘‘Coordinated voltage control in offshore HVDC connected cluster of wind power plants,’’ *IEEE Trans. Sustain. Energy*, vol. 7, no. 4, pp. 1592–1601, Oct. 2016, doi: 10.1109/TSTE.2016.2569430.

[6] A. Moawwad, M. S. El Moursi, andW. Xiao, ‘‘Advanced fault ride-through management scheme for VSC-HVDC connecting offshore wind farms,’’ *IEEE Trans. Power Syst.*, vol. 31, no. 6, pp. 4923–4934, Nov. 2016, doi: 10.1109/TPWRS. 2016.2535389.

[7] A. Moawwad, M. S. El Moursi, and W. Xiao, ‘‘A novel transient control strategy for VSC-HVDC connecting offshore wind power plant,’’ *IEEE Trans. Sustain. Energy*, vol. 5, no. 4, pp. 1056–1069, Oct. 2014, doi: 10.1109/TSTE.2014.2325951.

[8] A. Egea-Àlvarez, M. Aragüés-Peñalba, E. Prieto-Araujo, and O. Gomis- Bellmunt, ‘‘Power reduction coordinated scheme for wind power plants connected with VSC-HVDC,’’ *Renew. Energy*, vol. 107, pp. 1–13, Jul. 2017, doi: 10.1016/J.RENENE .2017.01.027.

[9] M. I. Hossain, M. Shafiullah, F. A. Al-Sulaiman, and M. A. Abido, ‘‘Comprehensive analysis of PV and wind energy integration into MMC-HVDC transmission network,’’ *Sustainability*, vol. 15, no. 1, p. 253, Dec. 2022, doi: 10.3390/ SU15010253.

[10] M. I. Hossain, M. A. Abido, and M. I. Pathan, ‘‘PMSG based wind energy integration into MMC based HVDC transmission network in RTDS,’’ in *Proc. IEEE Electr. Power Energy Conf. (EPEC)*, Nov. 2020, pp. 1–6, doi: 10.1109/EPEC48502. 2020.9320059.

[11] M. I. Hossain, M. A. Abido, and M. I. Pathan, ‘‘MMC based PV energy integrated multiterminal HVDC transmission network,’’ in *Proc. IEEE Electr. Power Energy Conf. (EPEC)*, Nov. 2020, pp. 1–6, doi:10.1109/EPEC48502.2020.9320120.

[12] S. Nanou and S. Papathanassiou, ‘‘Evaluation of a communication-based fault ride-through scheme for offshore wind farms connected through high-voltage DC links based on voltage source converter,’’ *IET Renew. Power Gener.*, vol. 9, no. 8, pp. 882–891, Nov. 2015, doi: 10.1049/ietrpg. 2015.0017.

[13] M. Ndreko, M. Popov, and M. A. M. M. van der Meijden, ‘‘Study on FRT compliance of VSC-HVDC connected offshore wind plants during AC faults including requirements for

ISSN 2249-3352 (P) 2278-0505 (E)

Cosmos Impact Factor-5.86

the negative sequence current control,'' *Int. J. Electr. Power Energy Syst.*, vol. 85, pp. 97–116, Feb. 2017, doi: 10.1016/J.IJEPES. 2016.08.009.

[14] S. I. Nanou, G. N. Patsakis, and S. A. Papathanassiou, ''Assessment of communication-independent grid code compatibility solutions for VSC–HVDC connected offshore wind farms,'' *Electr. Power Syst. Res.*, vol. 121, pp. 38–51, Apr. 2015, doi: 10.1016/J.EPSR.2014.12.002.

[15] M. Mohammadi, M. Avendano-Mora, M. Barnes, and J. Y. Chan, ''A study on fault ride-through of VSC-connected offshore wind farms,'' in *Proc. IEEE Power Energy Soc. Gen. Meeting*, Mar. 2013, p. 1–4, doi: 10.1109/PESMG.2013.6672514.

[16] O. D. Adeuyi, M. Cheah-Mane, J. Liang, L. Livermore, and Q. Mu, ''Preventing DC over-voltage in multi-terminal HVDC transmission,'' *CSEE J. Power Energy Syst.*, vol. 1, no. 1, pp. 86–94, Mar. 2015, doi: 10.17775/CSEEJPES.2015.00011.

[17] O. Gomis-Bellmunt, A. Egea-Alvarez, A. Junyent-Ferre, J. Liang, J. Ekanayake, and N. Jenkins, ''Multiterminal HVDC-VSC for offshore wind power integration,'' in *Proc. IEEE Power Energy Soc. Gen. Meeting*, Jul. 2011, pp. 1–6, doi: 10.1109/ PES.2011.6039238.

[18] R. Chen, K. Jia, T. Bi, B. Liu, and Y. Sun, ''Coordinated fault ride through strategy for offshore wind integration system,'' *IOP Conf. Ser. Earth Environ. Sci.*, vol. 170, no. 4, p. 42124, Jul. 2018, doi: 10.1088/1755- 1315/170/4/042124.

[19] A. Arulampalam, G. Ramtharan, N. Caliao, J. B. Ekanayake, and N. Jenkins, ''Simulated onshore-fault ride through of offshore wind farms connected through VSC HVDC,'' *Wind Eng.*, vol. 32, no. 2, pp. 103–114, Mar. 2008, doi: 10.1260/ 030952408784815781.

[20] M. Ndreko, A. Bucurenciu, M. Popov, and M. A. M. M. van der Meijden, ''On grid code compliance of offshore MTDC grids: Modeling and analysis,'' in *Proc. IEEE Eindhoven PowerTech*, Jun. 2015, pp. 1–6, doi: 10.1109/PTC.2015.7232398.

[21] Y. Yu, Z. Xu, and T. An, ''Fault ride-through strategy for fully rated converter wind turbines connected to the grid via MMC-HVDC transmission,'' in *Proc. 12th IET Int. Conf. AC DC Power Transmiss. (ACDC)*, 2016, p. CP696, doi: 10.1049/CP.2016.0406.

[22] J. Liang, O. Gomis-Bellmunt, J. Ekanayake, N. Jenkins, and W. An, ''A multi-terminal HVDC transmission system for offshore wind farms with induction generators,'' *Int. J. Electr. Power Energy Syst.*, vol. 43, no. 1, pp. 54–62, Dec. 2012, doi: 10.1016/j.ijepes.2012.04.063.

[23] W. Sun, R. E. Torres-Olguin, and O. Anaya-Lara, ''Investigation on fault-ride through methods for VSC-HVDC connected offshore wind farms,'' *Energy Proc.*, vol. 94, pp. 29–36, Sep. 2016, doi: 10.1016/J.EGYPRO.2016.09.185.

[24] I. Erlich, C. Feltes, and F. Shewarega, ''Enhanced voltage drop control by VSC–HVDC systems for improving wind farm fault ridethrough capability,'' *IEEE Trans. Power Del.*, vol. 29, no. 1, pp. 378–385, Feb. 2014, doi: 10.1109/TPWRD.2013 .2285236.

[25] Y. Jing, R. Li, L. Xu, and Y. Wang, ''Enhanced AC voltage and frequency control on offshoreMMCstation for wind farm,'' *J. Eng.*, vol. 2017, no. 13, pp. 1264–1268, Jan. 2017, doi: 10.1049/JOE.2017.0532.

ISSN 2249-3352 (P) 2278-0505 (E)

Cosmos Impact Factor-5.86

[26] U. Karaagac, J. Mahseredjian, L. Cai, and H. Saad, ‘‘Offshore wind farm modeling accuracy and efficiency in MMC-based multiterminal HVDC connection,’’ *IEEE Trans. Power Del.*, vol. 32, no. 2, pp. 617–627, Apr. 2017, doi: 10.1109/TPWRD. 2016.2522562.

[27] M. C. Nguyen, K. Rudion, and Z. A. Styczynski, ‘‘Improvement of stability assessment of VSCHVDC transmission systems,’’ in *Proc. 5th Int. Conf. Crit. Infrastruct. (CRIS)*, Sep. 2010, pp. 1–10, doi: 10.1109/CRIS.2010.5617545.

[28] L. Xu, L. Yao, and C. Sasse, ‘‘Grid integration of large DFIG-based wind farms using VSC transmission,’’ *IEEE Trans. Power Syst.*, vol. 22, no. 3, pp. 976–984, Aug. 2007, doi: 10.1109/TPWRS.2007.901306.

[29] X. Hu, J. Liang, D. J. Rogers, and Y. Li, ‘‘Power flow and power reduction control using variable frequency of offshore AC grids,’’ *IEEE Trans. Power Syst.*, vol. 28, no. 4, pp. 3897–3905, Nov. 2013, doi:10.1109/TPWRS.2013.2257884.

[30] B. Silva, C. L. Moreira, H. Leite, and J. A. Pecas Lopes, ‘‘Control strategies for AC fault ride through in multiterminal HVDC grids,’’ *IEEE Trans. Power Del.*, vol. 29, no. 1, pp. 395–405, Feb. 2014, doi:10.1109/TPWRD.2013.2281331.

[31] O. Goksu, R. Teodorescu, C. L. Bak, F. Iov, and P. C. Kjaer, ‘‘Instability of wind turbine converters during current injection to low voltage grid faults and PLL frequency based stability solution,’’ *IEEE Trans. Power Syst.*, vol. 29, no. 4, pp. 1683–1691, Jul. 2014, doi:10.1109/TPWRS.2013.2295261.

[32] M. Aragues Penalba, O. Gomis-Bellmunt, and M. Martins, ‘‘Coordinated control for an offshore wind power plant to provide fault ride through capability,’’ *IEEE Trans. Sustain. Energy*, vol. 5, no. 4, pp. 1253–1261, Oct. 2014, doi: 10.1109/TSTE. 2014.2344172.

[33] S. Ma, H. Geng, L. Liu, G. Yang, and B. C. Pal, ‘‘Grid-synchronization stability improvement of large scale wind farm during severe grid fault,’’ *IEEE Trans. Power Syst.*, vol. 33, no. 1, pp. 216–226, Jan. 2018, doi:10.1109/TPWRS.2017.2700050.

[34] W. Li, M. Zhu, P. Chao, X. Liang, and D. Xu, ‘‘Enhanced FRT and postfault recovery control for MMC-HVDC connected offshore wind farms,’’ *IEEE Trans. Power Syst.*, vol. 35, no. 2, pp. 1606–1617, Mar. 2020, doi: 10.1109/TPWRS. 2019.2944940.

[35] *Battery Storage for Renewables: Market Status and Technology Outlook*. Accessed: Jan. 27, 2022. [Online]. Available: http://publications/2015/Jan/Battery-Storage-for-Renewables-Market- Status-and-Technology-Outlook

[36] *CNESA Global Energy Storage Market Analysis—2020.Q1 (Summary)—China Energy Storage Alliance*. Accessed: Jan. 27, 2022. [Online]. Available: http://en.cnesa.org/latest-news/2020/5/28/cnesa-global-energy-storage-market analysis - 2020q1-summary

[37] M. Y. Suberu, M. W. Mustafa, and N. Bashir, ‘‘Energy storage systems for renewable energy power sector integration and mitigation of intermittency,’’ *Renew. Sustain. Energy Rev.*, vol. 35, pp. 499–514, Jul. 2014, doi: 10.1016/j.rser.2014. 04.009.

[38] H. Chen, T. N. Cong, W. Yang, C. Tan, Y. Li, and Y. Ding, ‘‘Progress in electrical energy storage system: A critical review,’’ *Prog. Natural Sci.*, vol. 19, no. 3, pp. 291–312, Mar. 2009, doi: 10.1016/j.pnsc.2008. 07.014.

ISSN 2249-3352 (P) 2278-0505 (E)

Cosmos Impact Factor-5.86

[39] S. D. Ahmed, F. S. M. Al-Ismail, M. Shafiullah, F. A. Al-Sulaiman, and I. M. El-Amin, ‘‘Grid integration challenges of wind energy: A review,’’ *IEEE Access*, vol. 8, pp. 10857–10878, 2020, doi:10.1109/ACCESS.2020.2964896.

[40] M. Shafiullah, S. D. Ahmed, and F. A. Al-Sulaiman, ‘‘Grid integration challenges and solution strategies for solar PV systems: A review,’’ *IEEE Access*, vol. 10, pp. 52233–52257, 2022, doi: 10.1109/ACCESS.2022.3174555.

[41] M. Ali, M. I. Hossain, and M. Shafiullah, ‘‘Fuzzy logic for energy management in hybrid energy storage systems integrated DC microgrid,’’ in *Proc. Int. Conf. Power Energy Syst. Appl. (ICoPESA)*, Feb. 2022, pp. 424–429, doi: 10.1109/ ICOPESA54515.2022.9754406.

[42] M. I. Hossain, M. Shafiullah, and M. A. Abido, ‘‘Battery power control strategy for intermittent renewable energy integrated modular multilevel converter-based high-voltage direct current network,’’ *Sustainability*, vol. 15, no. 3, p. 2626, Feb. 2023, doi: 10.3390/SU15032626.

[43] M. N. Hellesnes, K. Sharifabadi, and S. A. S. S. Acevedo. (2017). *Use of Battery Energy Storage for Power Balancing in a Large- Scale HVDC Connected Wind Power Plant*. NTNU. [Online]. Available: https://ntnuopen.ntnu.no/ntnu-xmlui/ handle/ 11250/2454582

[44] I. P. Reite. (2017). *Battery Energy Storage System Connected to a Three-Phase 50 Hz-Grid*. NTNU. [Online]. Available: https://ntnuopen.ntnu.no/ntnu-xmlui/handle/ 11250/2453622

[45] Y. Ma, H. Lin, Z. Wang, and Z. Ze, ‘‘Modified state-of-charge balancing control of modular multilevel converter with integrated battery energy storage system,’’ *Energies*, vol. 12, no. 1, p. 96, Dec. 2018, doi:10.3390/en12010096.

[46] G. Wang, G. Konstantinou, C. D. Townsend, J. Pou, S. Vazquez, G. D. Demetriades, and V. G. Agelidis, ‘‘A review of power electronics for grid connection of utility-scale battery energy storage systems,’’ *IEEE Trans. Sustain. Energy*, vol. 7, no. 4, pp. 1778–1790, Oct. 2016, doi:10.1109/TSTE.2016.2586941.

[47] T. Soong and P. W. Lehn, ‘‘Evaluation of emerging modular multilevel converters for BESS applications,’’ *IEEE Trans. Power Del.*, vol. 29, no. 5, pp. 2086–2094, Oct. 2014, doi: 10.1109/TPWRD.2014.2341181.

[48] M. Hagiwara and H. Akagi, ‘‘Control and experiment of pulsewidth-modulated modular multilevel converters,’’ *IEEE Trans. Power Electron.*, vol. 24, no. 7, pp. 1737–1746, Jul. 2009, doi:10.1109/TPEL.2009.2014236.

[49] B. Xiao, F. Filho, and L. M. Tolbert, ‘‘Single-phase cascaded H-bridge multilevel inverter with nonactive power compensation for gridconnected photovoltaic generators,’’ in *Proc. IEEE Energy Convers. Congr. Expo.*, Sep. 2011, pp. 2733–2737, doi: 10.1109/ECCE.2011.6064135.

[50] Q. Chen, R. Li, and X. Cai, ‘‘Analysis and fault control of hybrid modular multilevel converter with integrated battery energy storage system,’’ *IEEE J. Emerg. Sel. Topics Power Electron.*, vol. 5, no. 1, pp. 64–78, Mar. 2017, doi: 10.1109 /JESTPE.2016.2623672.

ISSN 2249-3352 (P) 2278-0505 (E)
Cosmos Impact Factor-5.86

[51] A. Lachichi, ‘‘Modular multilevel converters with integrated batteries energy storage,’’ in *Proc. Int. Conf. Renew. Energy Res. Appl. (ICRERA)*, Oct. 2014, pp. 828–832, doi: 10.1109/ICRERA.2014.7016501.
[52] I. Trintis, S. Munk-Nielsen, and R. Teodorescu, ‘‘A new modular multilevel converter with integrated energy storage,’’ in *Proc. 37th Annu. Conf. IEEE Ind. Electron. Soc.*, Nov. 2011, pp. 1075–1080, doi:10.1109/IECON.2011.6119457.
[53] T. Soong. (2015). *Modular Multilevel Converters With Integrated Energy Storage*. [Online]. Available: https://tspace.library.utoronto.ca/handle/1807/71617
[54] F. Nadeem, S. M. S. Hussain, P. K. Tiwari, A. K. Goswami, and T. S. Ustun, ‘‘Comparative review of energy storage systems, their roles, and impacts on future power systems,’’ *IEEE Access*, vol. 7, pp. 4555–4585, 2019, doi: 10.1109/ ACCESS.2018.2888497.
[55] M. C. Argyrou, P. Christodoulides, and S. A. Kalogirou, ‘‘Energy storage for electricity generation and related processes: Technologies appraisal and grid scale applications,’’ *Renew. Sustain. Energy Rev.*, vol. 94, pp. 804–821, Oct. 2018, doi: 10.1016/j.rser.2018.06.044.
[56] M. Swierczynski, R. Teodorescu, C. N. Rasmussen, P. Rodriguez, and H. Vikelgaard, ‘‘Overview of the energy storage systems for wind power integration enhancement,’’ in *Proc. IEEE Int. Symp. Ind. Electron.*, Jul. 2010, pp. 3749–3756, doi: 10.1109/ISIE.2010.5638061.
[57] S. R. Salkuti and C. M. Jung, ‘‘Comparative analysis of storage techniques for a grid with renewable energy sources,’’ *Int. J. Eng. Technol.*, vol. 7, no. 3, pp. 970–976, Jun. 2018, doi: 10.14419/ijet.v7i3.12728.
[58] M. Ahmed, S. Kuriry, M. D. Shafiullah, and M. A. Abido, ‘‘DC microgrid energy management with hybrid energy storage systems,’’ in *Proc. 23rd Int. Conf. Mechatronics Technol. (ICMT)*, Oct. 2019, pp. 1–6, doi: 10.1109/ICMECT.2019 .8932147.
[59] P. F. Ribeiro, B. K. Johnson, M. L. Crow, A. Arsoy, and Y. Liu, ‘‘Energy storage systems for advanced power applications,’’ *Proc. IEEE*, vol. 89, no. 12, pp. 1744–1756, 2001, doi: 10.1109/5.975900.
[60] Z. Chen, X. Zou, S. Duan, and H. Wei, ‘‘Power conditioning system of flywheel energy storage,’’ in *Proc. 8th Int. Conf. Power Electron.*, May 2011, pp. 2763–2768, doi: 10.1109/ICPE.2011.5944769.
[61] M. Amiryar and K. Pullen, ‘‘A review of flywheel energy storage system technologies and their applications,’’ *Appl. Sci.*, vol. 7, no. 3, p. 286, Mar. 2017, doi: 10.3390/APP7030286.
[62] F. Diaz-Gonzalez, A. Sumper, O. Gomis-Bellmunt, and R. Villafafila-Robles, ‘‘Modeling and validation of a flywheel energy storage lab-setup,’’ in *Proc. 3rd IEEE PES Innov. Smart Grid Technol. Eur.*, Oct. 2012, pp. 1–12, doi: 10.1109/ISGTEUROPE.2012.6465640.
[63] G. Nair S and N. Senroy, ‘‘Power smoothening using multi terminal DC based DFIG connection and flywheel energy storage system,’’ in *Proc. IEEE 6th Int. Conf. Power Syst. (ICPS)*, Mar. 2016, pp. 1–6, doi: 10.1109/ICPES.2016.7584134.

ISSN 2249-3352 (P) 2278-0505 (E)

Cosmos Impact Factor-5.86

[64] R. G. Gadelrab, M. S. Hamad, A. S. Abdel-Khalik, and A. E. Zawawi, ‘‘Wind farms-fed HVDC system power profile enhancement using solid state transformer based flywheel energy storage system,’’ *J. Energy Storage*, vol. 4, pp. 145–155, Dec. 2015, doi: 10.1016/j.est.2015.10.003.

[65] M. I. Daoud, A. M. Massoud, A. S. Abdel-Khalik, A. Elserougi, and S. Ahmed, ‘‘A flywheel energy storage system for fault ride through support of grid-connected VSC HVDC-based offshore wind farms,’’ *IEEE Trans. Power Syst.*, vol. 31, no. 3, pp. 1671–1680, May 2016, doi:10.1109/TPWRS.2015.2465163.

[66] K. H. Ahmed, A. S. Abdel-Khalik, A. Elserougi, A. Massoud, and S. Ahmed, ‘‘Fault ride-through capability enhancement based on flywheel energy storage system for wind farms connected via VSC high voltage DC transmission,’’ in *Proc. 10th IET Int. Conf. AC DC Power Transmiss.(ACDC)*, 2012, pp. 1–13, doi: 10.1049/cp.2012.1988.

[67] I. A. Gowaid, A. A. Elserougi, A. S. Abdel-Khalik, A. M. Massoud, and S. Ahmed, ‘‘A series flywheel architecture for power levelling and mitigation of DC voltage transients in multi-terminal HVDC grids,’’ *IET Gener., Transmiss. Distrib.*, vol. 8, no. 12, pp. 1951–1959, Dec. 2014, doi:1 10.1049/iet-gtd.2013.0953.

[68] M. I. Daoud, A. Massoud, S. Ahmed, A. S. Abdel-Khalik, and A. Elserougi, ‘‘Ride-through capability enhancement of VSC-HVDC based wind farms using low speed flywheel energy storage system,’’ in *Proc. IEEE Appl. Power Electron. Conf. Expo.*, Mar. 2014, pp. 2706–2712, doi: 10.1109/APEC.2014.6803687.

[69] M. I. Daoud, A. Massoud, A. Elserougi, A. Abdel-Khalik, and S. Ahmed, ‘‘A dual three-phase induction machine based flywheel storage system driven by modular multilevel converters for fault ride through in HVDC systems,’’ in *Proc. IEEE PES Asia–Pacific Power Energy Eng. Conf. (APPEEC)*, Nov. 2015, pp. 1–5, doi: 10.1109/ APPEEC.2015.7380870.

[70] L.Yang, Z. Xu, J. Ostergaard, Z.Y. Dong, and K. P.Wong, ‘‘Advanced control strategy of DFIG wind turbines for power system fault ride through,’’ *IEEE Trans. Power Syst.*, vol. 27, no. 2, pp. 713–722, May 2012, doi: 10.1109/TPWRS.2011. 2174387.

[71] X. Zeng, T. Liu, S. Wang, Y. Dong, and Z. Chen, ‘‘Comprehensive coordinated control strategy of PMSG-based wind turbine for providing frequency regulation services,’’ *IEEE Access*, vol. 7, pp. 63944–63953, 2019, doi: 10.1109/ACCESS.2019. 2915308.

[72] K. S. Tey and S. Mekhilef, ‘‘Modified incremental conductance MPPT algorithm to mitigate inaccurate responses under fast-changing solar irradiation level,’’ *Sol. Energy*, vol. 101, pp. 333–342, Mar. 2014, doi:10.1016/J.SOLENER.2014.01.003.

[73] S. Motahhir, A. El Hammoumi, and A. El Ghzizal, ‘‘The most used MPPT algorithms: Review and the suitable low-cost embedded board for each algorithm,’’ *J. Cleaner Prod.*, vol. 246, Feb. 2020, Art. no. 118983, doi:10.1016/J.JCLEPRO. 2019.118983.